Modal Phenomena in the Natural Electromagnetic Spectrum Below 5 kHz

Dana Porrat*
Peter R. Bannister†
Antony C. Fraser-Smith*

January 30, 2001

*D. Porrat and A. C. Fraser-Smith are with the STAR Laboratory, Stanford University, Stanford, California 94305, USA. dporrat@wireless.stanford.edu, acfs@stanford.edu.

†P. R. Bannister is at 154 Nebraska Circle, Sebastian, Florida, USA.

Abstract

This paper presents new measurements of the magnetic field component of naturally–produced electromagnetic radiation in the ELF/VLF range. The measurements are compared to calculations based on modal propagation theory. The nocturnal spectrum below 5 kHz often contains a sharp increase in spectral level at the cutoff frequency of the first mode (∼1700 Hz), and a distinct variation of the spectral behavior at the cutoff frequency of the second mode (∼3400 Hz), where the indicated cutoff frequencies were calculated for perfectly conducting earth and ionosphere, with the ionosphere 88 km above the earth. These features are attributed to an enhancement in the first (QTE_1) and second (QTE_2) propagating modes at night, which makes their level comparable to the basic (TEM) mode.

Another spectral feature, which also prevails during the night, is semi-periodic fluctuations of the spectrum between the two cutoff frequencies, with a short period at the low end of the band and a gradual increase of the period as frequency increases. A similar semi-periodic fluctuation is apparent above the cutoff frequency of the second mode up to the limit of the measured band at 5 kHz. These semi-periodic fluctuations of the spectrum are related to the modal nature of the electromagnetic wave propagation. We show that computations of the spectrum of the ELF/VLF radiation emitted by a vertical lightning in the earth–ionosphere waveguide gives spectra that compare well with

the measurements.

1 Introduction

The earth–ionosphere cavity has been modeled as waveguide for propagating radio waves by many authors, most notably Wait [1962] and Galejs [1972]. The common approach is to develop the modal theory and then argue that only the transverse electro–magnetic (TEM) mode propagates to significant distances in the Extremely Low Frequency (ELF; 3 Hz – 3 kHz) band and the lower end of the Very Low Frequency (VLF; 3 – 30 kHz) band. Experimental verification of the assumption that the higher modes (other than TEM) do not propagate to large distances is scarce since it is difficult to separate the effects of the various modes in measurement. Equipment and computational limitations at the time when most of the theoretical work in this field was done prevented a high resolution examination of the ELF/VLF spectrum near the waveguide cutoff frequencies [*Barr*, 1970].

This paper presents spectra measured in the ELF/VLF bands (500 Hz – 5000 Hz) that appear to contain modal features. The measured spectra are compared to calculations containing the three lowest modes of propagation and the similarities between theory and measurement are shown. The diurnal variation of the measured spectra and the effect of the source–observer distance are discussed.

Propagation theory is reviewed in section 2. An expression is presented for the magnetic field radiated by a vertical electric dipole source. Section 3

presents the measurements and compares them to the theoretical predictions.

2 Theory

This section resents the horizontal magnetic field radiated from a vertical source in the earth–ionosphere waveguide. A perfectly conducting waveguide model is discussed in 2.1 and the effects of the lossy ionosphere are presented in 2.2.

2.1 Propagation in a Perfectly Conducting Waveguide

The simplest model of the earth–ionosphere waveguide consists of a planar waveguide (the curvature of the earth neglected) with infinitely conducting walls; the effects of the earth's magnetic field are neglected. The vertical component of the electric field generated in this waveguide by a vertical electric dipole was described by [*Wait*, 1962]:

$$E_z = \frac{\mu_0 \omega I ds}{4h} \sum_{n=0,1,2,\ldots}^{\infty} \delta_n S_n^2 H_0^{(2)}(kS_n\rho)\cos(kC_n z_0)\cos(kC_n z) \qquad (1)$$

where a cylindrical coordinate system (ρ, ϕ, z) was used (fig. 1):

$\mu_0 = 4\pi \times 10^{-7}\ \frac{H}{m}$ is the permeability of free space;

$\omega = 2\pi f$ is the radial frequency;

I is the source current (assumed uniform over the source);

ds is the source length;

h is the waveguide height;

$\delta_0 = 1$, $\delta_n = 2$ for $n > 0$;

$H_0^{(2)}(\cdot)$ is the Hankel function of the second kind of the 0^{th} order;

$k = \frac{\omega}{c}$ is the wavenumber in free space;

$c = 3 \times 10^8 \ \frac{m}{s}$ is the speed of light;

$C_n = \cos(\theta_n)$ is the cosine of the eigenangle for the n^{th} mode. θ_n is the eigenangle of the n^{th} mode, shown in figure 1;

$S_n = \sin(\theta_n) = \sqrt{1 - C_n^2}$ is the sine of the eigenangle for the n^{th} mode;

ρ is the horizontal separation between the source and the observation point;

z_0 is the source height above earth

and z is the height of the observation point above earth.

Equation (1) is a summation over Transverse Magnetic (TM) modes, where the magnetic field is transverse to the plane of incidence of the wave on the waveguide walls. Each mode is characterized by its order n, and is thus named TM_n. Equation (1) is a phasor representation of the field, where an $e^{i\omega t}$ time variation is assumed. For large enough separations between the source and the observation point ($|kS_n\rho| > 2$), the Hankel function in (1) can be approximated by an exponential. Another simplification is taken by considering low source and receiver i.e., z, $z_0 \ll \lambda$ (where λ is the wavelength). In our model $z, z_0 < \frac{1}{10}\lambda$, so we can neglect the cosine factors in (1) and the

field expression becomes:

$$E_z = \frac{E_0}{2}\frac{(\rho/\lambda)^{1/2}}{(h/\lambda)}e^{i[k\rho-\pi/4]}\sum_{n=0}^{\infty}\delta_n S_n^{3/2}e^{-ikS_n\rho} \tag{2}$$

where

$E_0 = i\frac{\eta}{\lambda}Ids\frac{e^{-ik\rho}}{\rho}$;

$\eta = \sqrt{\frac{\mu_0}{\epsilon_0}} \simeq 120\pi\ \Omega$ is the free space impedance

and $\epsilon_0 = 8.85 \times 10^{-12}\ \frac{F}{m}$ is the free space permitivity.

The far field approximation is valid roughly where $\rho > 3h$ and $\rho > 2\lambda$, which for $\rho \geq$1000 km holds for frequencies higher than 600 Hz.

The magnetic field in a cylindrical coordinate system is described by:

$$H_\phi = -\frac{E_0}{2\eta}\frac{(\rho/\lambda)^{1/2}}{(h/\lambda)}e^{i[k\rho-\pi/4]}\sum_{n=0}^{\infty}\delta_n S_n^{1/2}e^{-ikS_n\rho} \tag{3}$$

The fields generated by a horizontal electrical dipole were also considered, but they are significantly weaker than the fields generated by a vertical source because of the low impedance presented by the waveguide for horizontal sources at low altitudes [*Sukhorukov*, 1996]. These field components are not considered in the following computation.

Each mode is characterized by a cutoff frequency, above which it is able to propagate. The Transverse Electro-Magnetic or TEM mode ($n = 0$) propagates at any frequency, and therefore has a zero cutoff frequency $f_0 = 0$. For the higher order modes, the cutoff frequency in a planar perfectly conducting waveguide is $f_n = n\frac{c}{2h}$. For typical nighttime conditions (h =88 km), the

cutoff frequencies of the first TM modes are:

$$f_1 = 1700\ Hz \tag{4}$$

$$f_2 = 3400\ Hz \tag{5}$$

Modes of order $n = 3$ or higher are not considered because their cutoff frequencies are higher than our measurement limit of 5 kHz.

2.2 Propagation with a Lossy Ionosphere

In order to develop a more realistic propagation theory for ELF/VLF radiation in the earth–ionosphere waveguide, it was necessary to extend the model of the waveguide by considering a finite conductivity in the ionosphere.

A vertical electric dipole source excites TM waves as described earlier, but can also excite Quasi-Transverse Electric (QTE) modes [*Wait*, 1962; *Yamashita*, 1978; *Sukhorukov*, 1996]. The TM waves couple into QTE waves via ionospheric reflections; The mechanism involves the coupling of an incident TM wave into Right (R) and Left (L) modes in the ionosphere [*Stubbe et al.*, 1982]. The R and L waves travel within the ionosphere with different phase velocities and attenuation rates, they are reflected (towards the earth) at different altitudes. As the R and L waves propagate into the region below the ionosphere they form Quasi-Transverse Magnetic (QTM) and Quasi-Transverse Electric (QTE) components.

The coupling of QTM radiation into QTE radiation is stronger near the

cutoff frequencies of the earth–ionosphere waveguide than it is at other frequencies. It is the coupling of QTM modes into QTE modes that accounts for the similarity between the field expressions developed earlier for the TM modes (3) and the expressions for the QTE modes presented shortly (12). [*Yamashita*, 1978] and [*Sukhorukov*, 1996] show that when considering the coupling between QTM and QTE modes, at frequencies near cutoff, the ratio between the horizontal components of the magnetic field produced by a vertical electric dipole source is

$$\frac{|H_\rho|}{|H_\phi|} \simeq \tan\phi \tag{6}$$

where ϕ is the azimuthal angle. We conclude that a vertical electric dipole source radiating under a lossy ionosphere generates QTE waves with a significant magnetic component in the ϕ direction. For a more detailed discussion of the frequency dependent polarization of natural radiation in the ELF/VLF frequency bands, see [*Hayakawa et al.*, 1994].

The QTM waves are attenuated much more (tens of $\frac{dB}{Mm}$) than the QTE waves as they travel within the earth–ionosphere waveguide [*Yamashita*, 1978]. Therefore, in our 500 Hz to 5 kHz approximate analysis, we consider only the TEM and first two QTE_m modes (m=1,2).

We consider a lossy ionosphere which extends above altitude H. The conductivity of the ionosphere in this model is described by a single scale

height exponential profile [*Wait and Spies*, 1964].

$$\sigma(z) = 2.5 \times 10^5 \epsilon_0 e^{\frac{z-H}{\zeta_0}} = 2.5 \times 10^5 \epsilon_0 e^{\beta(z-H)} \tag{7}$$

where ζ_0 is the scale height and β is the inverse scale height. σ is measured in $Siemens/m$.

For such a profile, [*Greifinger and Greifinger*, 1978, 1979] have shown that the ELF propagation is characterized by three parameters: two altitudes and the scale height ζ_0. The lower altitude h_0 is the height at which the conduction current parallel to the magnetic field becomes equal to the displacement current (i.e., $\sigma(h_0) = \omega\epsilon_0$). The upper altitude h_1 is the height at which the local wave number becomes equal to the reciprocal of the local scale height of the refractive index (i.e. $4\omega\mu_0\sigma(h_1)\zeta_0^2 = 1$).

The altitudes h_0 and h_1 can easily be calculated from equation (7). The resulting expressions are

$$h_0 = H - \zeta_0 \ln\left(\frac{2.5 \times 10^5}{2\pi f}\right) \tag{8}$$

and

$$h_1 = h_0 + 2\zeta_0 \ln\left(\frac{2.39 \times 10^7}{f\zeta_0}\right) \tag{9}$$

where ζ_0 is given in meters and the frequency f is in Hertz.

In both ELF and VLF, the usual variation in β at night is 0.3 to 0.7 km^{-1},

and the usual variation in H at night is 80 to 95 km [*Bannister*, 1999; *Ferguson*, 1993; *Borgmann*, 1993].

The modal eigenvalues are approximated by

$$C_m = \frac{m\pi}{kh_1} \tag{10}$$

$$S_m = \sqrt{1 - C_m^2} \tag{11}$$

see [*Sukhorukov et al.*, 1992] for a detailed calculation of the eigenvalues for a lossy ionosphere model.

Using equation (3), the expression of the magnetic field can be written as:

$$H_\phi = -\frac{E_0}{2\eta} (\rho\lambda)^{1/2} e^{i[k\rho - \pi/4]} \left[\frac{S_0^{1/2}}{h_0} e^{-ikS_0\rho} e^{-\alpha_0\rho} + \sum_{m=1}^{2} \frac{\delta_m S_m^{1/2}}{h_1} e^{-ikS_m\rho} e^{-\alpha_m\rho} \right] \tag{12}$$

where δ_m are the excitation factors which describe the coupling of the source and receiving antennas to the earth–ionosphere waveguide, and α_m are the attenuation rates. These factors are now calculated.

2.2.1 Attenuation Rates

The attenuation rates α_m in (12) describe the attenuation of the propagating modes in the waveguide with increasing distances from the source.

The attenuation rate for the TEM mode is given by [*Greifinger and Greifinger*, 1978, 1979]:

$$\alpha_0 \simeq 0.143 f \frac{c}{v} \left(\frac{\zeta_0}{h_0} + \frac{\zeta_0}{h_1} \right) = 0.143 \frac{\zeta_0}{h_0} \frac{(c/v)^2 + 1}{c/v}$$

$$\simeq \quad 0.286 f \frac{\zeta_0}{h_0} = \frac{0.286 f}{\beta h_0} \quad \left[\frac{dB}{Mm}\right] \tag{13}$$

where $\frac{c}{v} \simeq \sqrt{\frac{h_1}{h_0}}$ is the TEM mode phase velocity ratio and the frequency f is measured in Hertz.

For the QTE modes, in the frequency range $f > \sqrt{2} f_m$ (where f_m is the cutoff frequency of mode m), the attenuation rate is given by [*Sukhorukov*, 1993]:

$$\alpha_m \simeq \frac{0.286 f}{\beta h_1} \left|\frac{C_m^2}{S_m}\right| \quad \left[\frac{dB}{Mm}\right] \tag{14}$$

For the frequency range $f_m + m \times 60\ Hz < f < \sqrt{2} f_m$, *Sukhorukov*'s [1996] equations can be modified to yield

$$\alpha_m \simeq \frac{0.286 f}{\beta h_1} |S_m| \quad \left[\frac{dB}{Mm}\right] \tag{15}$$

Note that α_0 is proportional to h_0^{-1}, while α_m is proportional to h_1^{-1}.

For frequencies below $f_m + m \times 60$ Hz we assumed a constant attenuation rate, equal to the attenuation rate calculated at $f_m + m \times 60$ Hz. This was done in order to smooth out the theoretical curves near the cutoff frequencies.

2.2.2 Excitation Factors

The excitation factors δ_0 and δ_m describe the coupling of the source and receiving antennas to the earth–ionosphere waveguide. [*Wheeler*, 1964] has shown that the excitation factors are directly related to the attenuation rates.

Therefore:

$$\delta_0 \simeq 1 \tag{16}$$

$$\delta_m \simeq \left|\frac{2C_m^2}{S_m}\right| \quad for\ f > \sqrt{2}f_m \tag{17}$$

and

$$\delta_m \simeq |2S_m| \quad for\ f_m + m \times 60\ Hz < f < \sqrt{2}f_m \tag{18}$$

For frequencies below $f_m + m \times 60$ Hz we assumed constant excitation factors, equal to the excitation factors calculated at $f_m + m \times 60$ Hz.

Note that both the attenuation rates and excitation factors of the QTE modes *increase* with frequency for $f < \sqrt{2}f_m$, and *decrease* with frequency for $f > \sqrt{2}f_m$. This increase and then decrease with frequency is in agreement with the calculations of [*Yamashita*, 1978], who employed a homogeneous anisotropic ionospheric model.

2.3 A Brief Summary of the Theory

The main result of section 2 is equation (12), which describes the horizontal component of the magnetic field radiated from a vertical lightning source. This expression is compared to measurements in section 3.

3 Measurements

ELF signals were recorded by the Stanford radiometer system [*Fraser-Smith and Helliwell*, 1994] during the months of September–November, 1999. The

system included a pair of loop antennas receiving the orthogonal components of the horizontal magnetic field. Measurements were taken twice per hour, where for each measurement the ELF/VLF spectra were averaged over a period of 2.5 minutes. The measured spectra show strong diurnal variations, which are demonstrated by comparing a typical night spectrum (figure 2) to a typical day spectrum (figure 3). The vertical lines in the measured spectra are caused by 60 Hz (power-line) harmonics. Only one component of the horizontal magnetic field is shown since the other component exhibits very similar trends.

We now proceed to inspect the modal features of the measured spectra and their diurnal variations.

3.1 Modal Cutoff

In order to investigate the cutoff of the QTE_1 mode, the spectral level below the cutoff (at 1490 Hz) and above it (at 2000 Hz) were averaged over 4 days. The results are plotted in figures 4 and 5 respectively.

The spectral level above the cutoff frequency (figure 5) presents a strong diurnal variation, where the nighttime level is about 25 dB above the daytime level. The spectral level below the modal cutoff (figure 4) shows a smaller diurnal variation, of the order of 10 dB.

The strong diurnal variation of the spectral level can also be appreciated by comparing the typical nighttime spectrum in figure 2 to the typical day-

time spectrum in figure 3, and noting the increase of spectral level in the nighttime spectrum above 1700 Hz. This jump in spectral level, which occurs at the cutoff frequency of the QTE_1 mode, is a very typical feature of the nighttime spectrum which occurs in about 90% of the measurements. A similar increase in spectral level occurs at the cutoff frequency of the QTE_2 mode, $f_2 = 3400$ Hz. This increase in spectral level is more gradual.

The increase in spectral levels above the cutoff frequencies of the QTE_1 and QTE_2 modes, which is present only in nighttime measurements, indicates that the propagation conditions of these modes (QTE_1 and QTE_2) go through a significant diurnal variation. The QTE_1 and QTE_2 modes appear to be very weak during the day (compared to the TEM mode), but they are significant during the night. The main reason for this change is the large difference in nighttime and daytime attenuation rates. For example, at a frequency of 2 kHz, the calculated nighttime value of α_1 is approximately 5 to 10 $\frac{dB}{Mm}$, while the measured daytime attenuation rate [*Bannister*, 1979; *Challinor*, 1967] is approximately 30 $\frac{dB}{Mm}$. For a range of 2 Mm, this 2 kHz attenuation rate difference translates to a 40 to 50 dB difference in field strengths.

3.2 Semi-periodic Spectral Fluctuations

Figure 6 presents a measured spectrum and a theoretical spectrum calculated from equation (12). The 60 Hz harmonics were removed from the measured spectrum using a median filter (which replaced each point by the median of

ten points around it); The spectrum was also smoothed in order to accentuate its dominant features. The theoretical spectrum was not smoothed and thus it contains fast variations which are absent from the measured curve. It was scaled so that it appears below the measured spectrum in the figure.

A semi-periodic feature is apparent in both the measured spectrum and the theoretical one at frequencies above 1700 Hz, the cutoff frequency of the QTE_1 mode. The fluctuations appear to have a small frequency width at low frequencies and they increase in width as the frequency increases. The period of the fluctuation increases between 1700 Hz and 3400 Hz and then goes through a second cycle of increase above 3400 Hz. While the dominant features of the theoretical graph agree with the measurement, the inconsistencies are attributed to inaccuracies of the model.

The semi-periodic fluctuations of the spectrum of a vertical source are the result of the modal summation and they can be explained by the difference of the rate of change of the phase for the different modes. The spectrum of each mode (12) is characterized by a phase factor $e^{-iS_n k\rho}$. The sum of any two modes generates a quasi-harmonic interference pattern in the spectrum, where the fluctuation depends on the modal eigenvalues, the frequency (through k), and the distance between the source and the receiver. It should be noted that the dependence of the spectrum of the different modes on the modal eigenvalues and on the frequency is complicated. The phase factor

$e^{-iS_n k\rho}$ has a considerable influence on the semi-periodic fluctuations, but their shape is also affected by other parts of the spectral expression (12).

Another example of the semi-periodic fluctuations is plotted in figure 7. In this example, the theoretical spectrum was calculated with the source located at a greater distance from the observation point (compared to the previous example in figure 6), which results is more rapid fluctuations of the spectrum.

Semi-periodic spectral fluctuations similar to the examples shown here, are apparent in approximately 30% of all the night measurements, and in none of the day measurements inspected.

The semi-periodic fluctuations of the nocturnal spectrum, which appear to be similar to the theoretical predictions based on the modal theory, suggest that the QTE_1 and QTE_2 modes are enhanced at night, compared to their daytime levels. It should be noted that the theoretical calculation are based on a single dipole source whose dipole moment is constant with frequency, which is a reasonable approximation of a single lightning at the relevant frequency range. We suggest that the semi-periodic fluctuations of the measured nocturnal spectrum are the effect of localized storms within the range of about 4000 km.

3.3 Attenuation Rates

The calculations of the modal attenuation rates and excitation factors (equations (14), (15), (17) and (18)) indicate a change in the characteristics of the propagation characteristics at $f = \sqrt{2}f_m$, where f_m are the cutoff frequencies of the different QTE modes. This variation in the spectrum is apparent in some measurements. Figure 8 presents such a measurement, where a distinct variation is evident near 2400 Hz (which approximately equals $\sqrt{2}f_1$). The figure also presents a theoretical spectrum, which contains a similar characteristic.

4 Conclusions

This paper presented the propagation theory in the ELF/VLF range (500 Hz – 5000 Hz) in the earth–ionosphere waveguide. In a waveguide with perfectly conducting walls, a vertical electric dipole source generates TM propagating modes, but when considering losses in the ionosphere, QTE modes are also generated.

Inspection of the ELF spectrum measured at night shows distinct modal features, which are not apparent in daytime measurements. A significant increase in spectral level occurs above 1700 Hz, the cutoff of the first quasi-transverse electric (QTE_1) mode. The spectral level goes through a diurnal variation of about 25 dB above the cutoff frequency. Another increase in

spectral level occurs at 3400 Hz, the cutoff of the second mode (QTE_2).

A second modal feature is semi-periodic fluctuations, which appear above the first cutoff and repeat above the second one. These fluctuations are very similar to the theoretical prediction, when the QTE_1 and QTE_2 modes are assumed to propagate with significant levels compared to the basic TEM mode.

These modal features of the nocturnal spectrum, which are completely missing in daytime measurement, indicate that the QTE_1 and QTE_2 modes propagate much better during the night than during the day. A difference in propagation conditions is also present for the TEM mode, but not to the same extent.

Acknowledgments

This work was supported in part by the High Frequency Active Auroral Research Program (HAARP), Air Force Research Laboratory, through contract No. F19628-96-C-0149, and in part by the Office of Naval Research through Grant No. N00014-92-J-1576.

The work of Dana Porrat was supported by the Stanford Graduate Fellowship.

The authors thank Jacob Bortnik for his advice and editorial comments.

References

[1] Peter R. Bannister. Some notes on ELF earth-ionosphere waveguide daytime propagation parameters. *IEEE Transactions on Antennas and Propagation*, AP-27(5):696–698, September 1979.

[2] Peter R. Bannister. Further examples of seasonal variations of ELF radio propagation parameters. *Radio Science*, 34(1):199–208, January-February 1999.

[3] R. Barr. The ELF and VLF amplitude spectrum of atmospherics with particular reference to the attenuation band near 3 kHz. *Journal of Atmospheric and Terrestrial Physics*, 32:977–990, 1970.

[4] Detlev Borgmann. Theoretical and experimental coverage analysis of a VLF transmitter. In *ELF/VLF/LF Radio Propagation and Systems Aspects AGARD-CP-529*, pages 6–1 – 6–5, 1993.

[5] R. A. Challinor. The phase velocity and attenuation of audio-frequency electromagnetic waves from simultaneous observations of atmospherics at two spaced stations. *Journal of Atmospheric and Terrestrial Physics*, 29:830–810, 1967.

[6] J. A. Ferguson. Numerical modeling of the propagation medium at VLF/LF. In *ELF/VLF/LF Radio Propagation and Systems Aspects AGARD-CP-529*, pages 1–1 – 1–9, 1993.

[7] Antony C. Fraser-Smith and Robert A. Helliwell. Overview of the Stanford University/Office of Naval Research ELF/VLF radio noise survey. In J. M. Goodman, editor, *Proceedings of the 1993 Ionospheric Effects Symposium*, pages 502–509, 1994.

[8] Janis Galejs. *Terrestrial Propagation of Long Electromagnetic Waves*. Pergamon Press, 1st edition, 1972.

[9] Carl Greifinger and Phyllis Greifinger. Approximate method for determining ELF eigenvalues in the earth-ionosphere waveguide. *Radio Science*, 13(5):831–837, September-October 1978.

[10] Carl Greifinger and Phyllis Greifinger. On the ionospheric parameters which govern high-latitude ELF propagation in the earth-ionosphere waveguide. *Radio Science*, 14:889–895, 1979.

[11] M. Hayakawa, K. Ohta, and K. Baba. Wave characteristics of tweek atmospherics deduced from the direction-finding measurement and theoretical interpretation. *Journal of Geophysical Reseach*, 99(D5):10,733–10,743, May 1994.

[12] P. Stubbe, H. Kopka, M. T. Rietveld, and R. L. Dowden. ELF and VLF wave generation by modulated HF heating of the current carrying lower ionosphere. *Journal of Atmospheric and Terrestrial Physics*, 44(12):1123–1135, 1982.

[13] A. I. Sukhorukov. Approximate solution for VLF propagation in an isotropic exponential earth-ionosphere waveguide. *Journal of Atmospheric and Terrestrial Physics*, 55(6):919–930, 1993.

[14] A. I. Sukhorukov. ELF-VLF atmospheric waveforms under night-time ionospheric conditions. *Annales Geophysicae*, 14:33–41, 1996.

[15] A. I. Sukhorukov, S. Shimakura, and M. Hayakawa. Approximate solution for the VLF eigenvalues near cut-off frequencies in the nocturnal inhomogeneous earth-ionosphere waveguide. *Planetary and Space Science*, 40(10):1363–1369, 1992.

[16] J. R. Wait and K. P. Spies. Characteristics of the earth-ionosphere waveguide for VLF radio waves. Technical Note 300, National Bureau of Standards, December 1964.

[17] James R. Wait. *Electromagnetic Waves in Stratified Media*. Pergamon Press, 1962. Reprinted 1996, IEEE Press.

[18] Harold A. Wheeler. VLF propagation under the ionosphere in the lowest mode of horizontal polarization. *Radio Science*, 68D(1):105–113, January 1964.

[19] Michiko Yamashita. Propagation of tweek atmospherics. *Journal of Atmospheric and Terrestrial Physics*, 40:151–156, 1978.

Figure 1: Geometry of the flat earth waveguide with a cylindrical coordinate system.

Figure 2: Measured spectrum on October 30, 1999, 08:00 UT (00:00 local), NS field component.

Figure 3: Measured Spectrum On October 26, 1999, 00:00 UT (16:00 local), NS field component.

Figure 4: Spectral level at 1490 Hz, (4 days averaged). The vertical bars indicate the standard deviation.

Figure 5: Spectral level at 2000 Hz, (4 days averaged). The vertical bars indicate the standard deviation.

Figure 6: Top: measured spectrum on October 30, 1999, 08:00 UT (00:00 local), NS field component; Bottom: Calculated spectrum of lower 3 modes, with ρ=1700 km, H=84 km, β=0.6 km^{-1}.

Figure 7: Top: measured spectrum on November 7, 1999, 10:00 UT (02:00 local), NS field component; Bottom: Calculated spectrum of lower 3 modes, with ρ=3200 km, H=84 km, β=0.7 km^{-1}.

Figure 8: Top: measured spectrum on October 27, 1999, 08:00 UT (00:00 local), NS field component; Bottom: Calculated spectrum of lower 3 modes, with ρ=3700 km, H=88 km, β=0.6 km^{-1}.

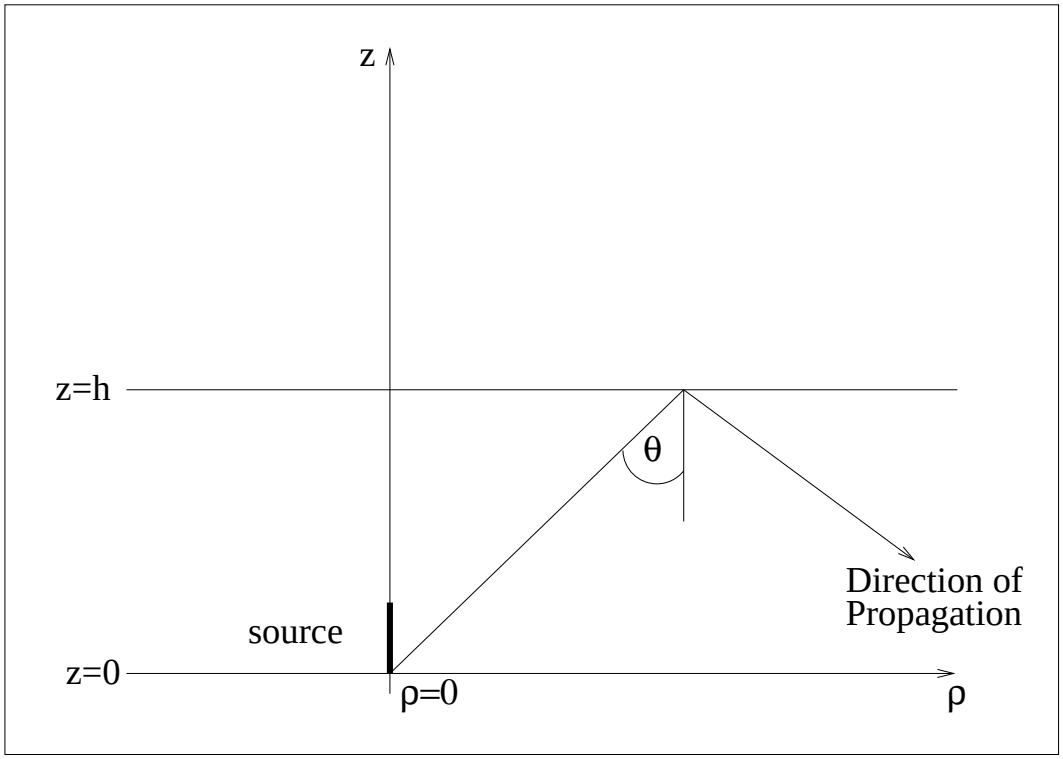

Figure 1:

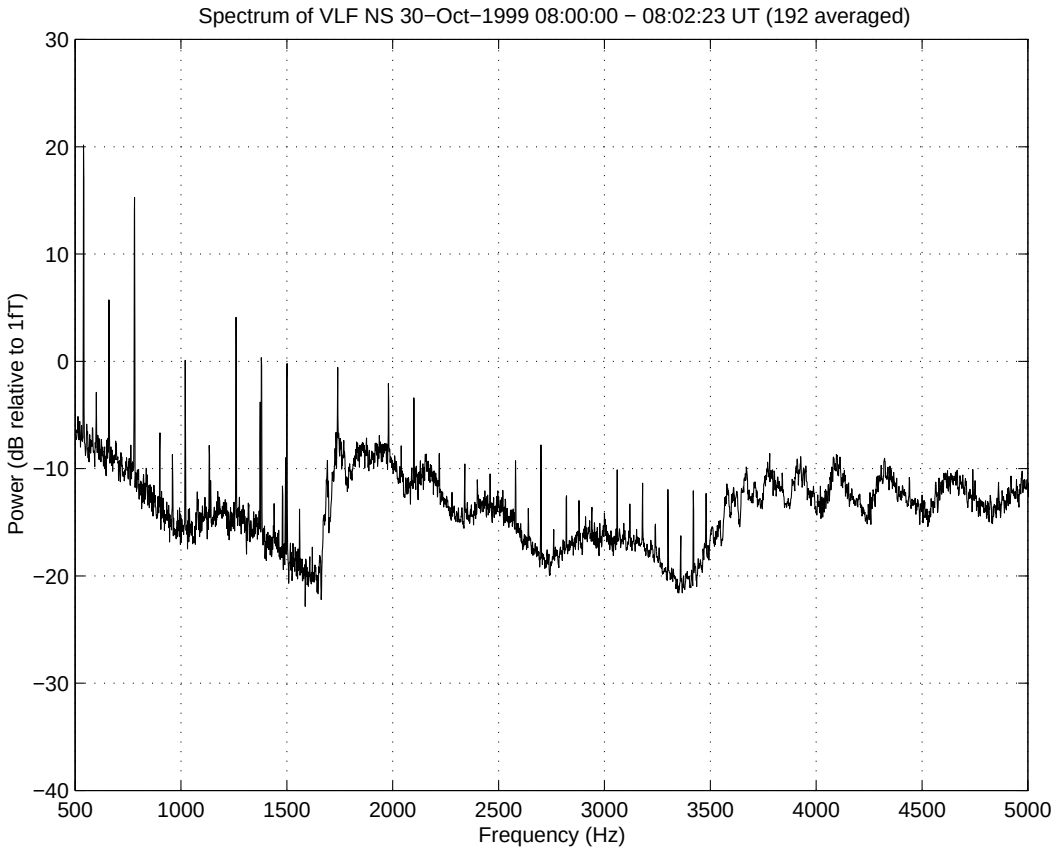
Spectrum of VLF NS 30−Oct−1999 08:00:00 − 08:02:23 UT (192 averaged)
Power (dB relative to 1fT)
Frequency (Hz)
30
20
10
0
−10
−20
−30
−40
500
1000
1500
2000
2500
3000
3500
4000
4500
5000

Figure 2:

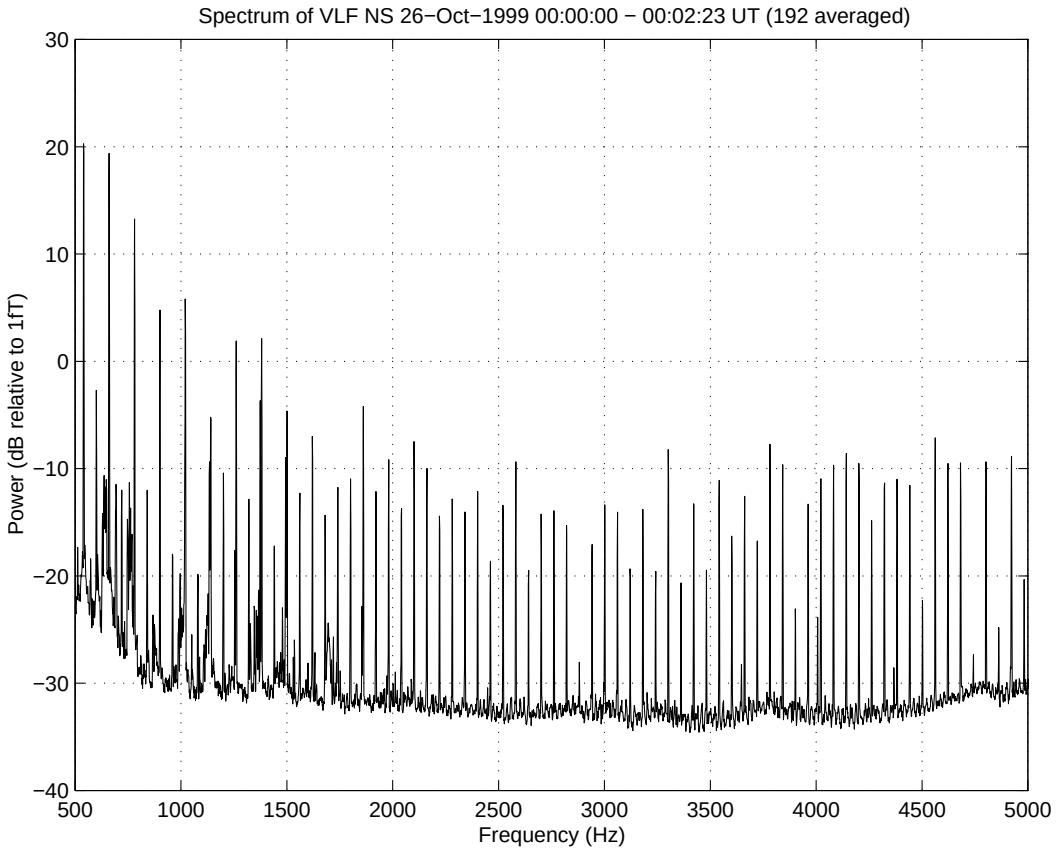
Spectrum of VLF NS 26−Oct−1999 00:00:00 − 00:02:23 UT (192 averaged)
Power (dB relative to 1fT)
Frequency (Hz)
30
20
10
0
−10
−20
−30
−40
500
1000
1500
2000
2500
3000
3500
4000
4500
5000

Figure 3:

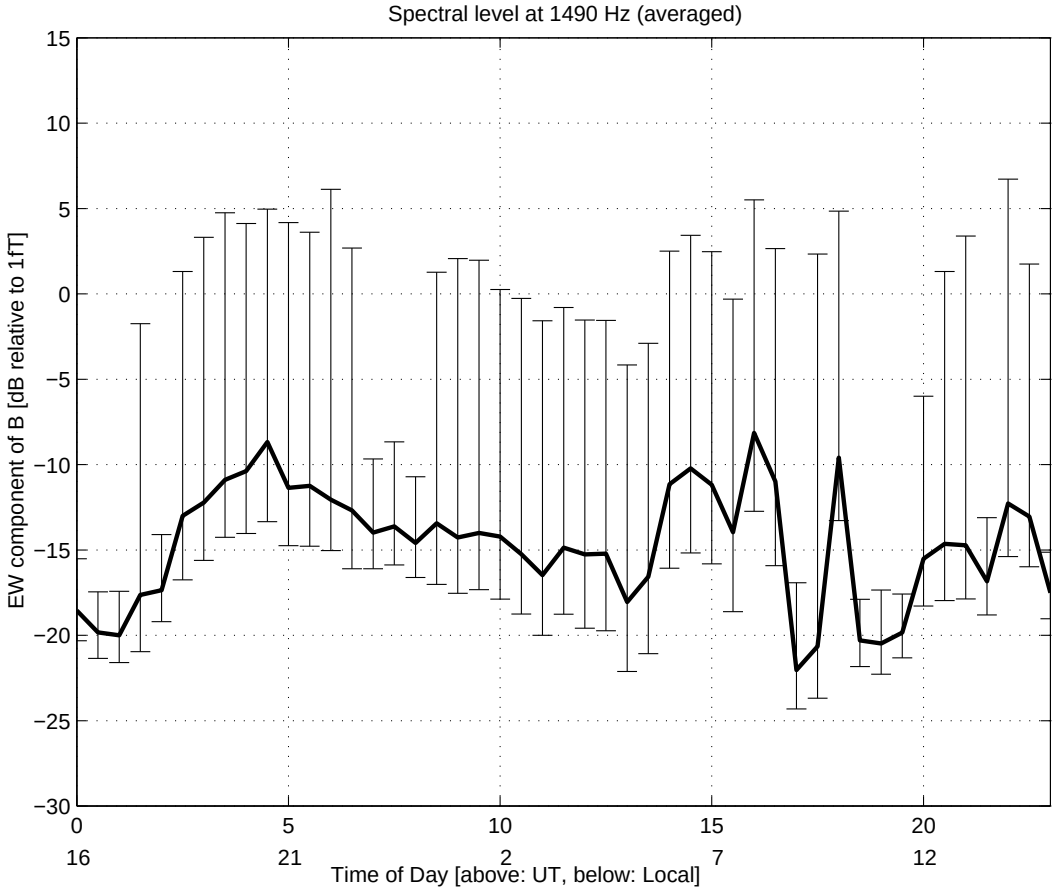
Spectral level at 1490 Hz (averaged)
EW component of B [dB relative to 1fT]
15
10
5
0
−5
−10
−15
−20
−25
−30
0
5
10
15
20
16
21
2
7
12
Time of Day [above: UT, below: Local]

Figure 4:

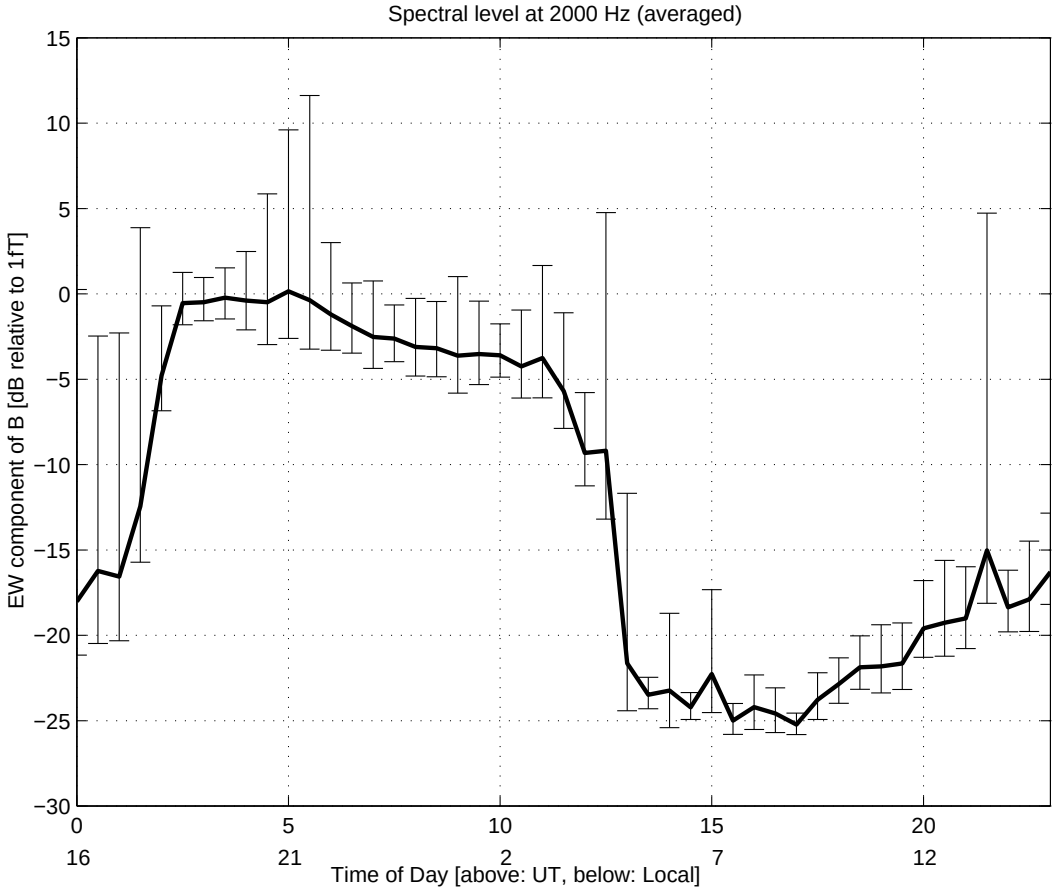
Spectral level at 2000 Hz (averaged)
EW component of B [dB relative to 1fT]
15
10
5
0
−5
−10
−15
−20
−25
−30
0
5
10
15
20
16
21
2
7
12
Time of Day [above: UT, below: Local]

Figure 5:

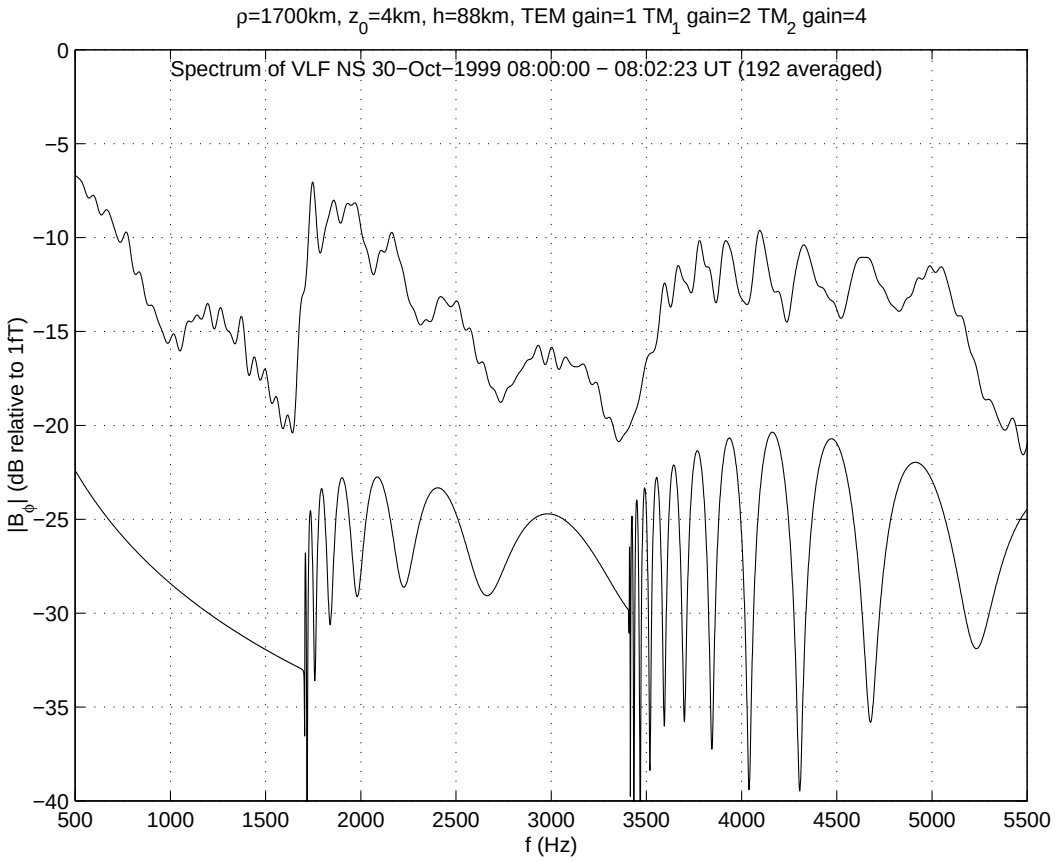
ρ=1700km, z0=4km, h=88km, TEM gain=1 TM1 gain=2 TM2 gain=4
Spectrum of VLF NS 30−Oct−1999 08:00:00 − 08:02:23 UT (192 averaged)
|Bφ| (dB relative to 1fT)
f (Hz)
0
−5
−10
−15
−20
−25
−30
−35
−40
500
1000
1500
2000
2500
3000
3500
4000
4500
5000
5500

Figure 6:

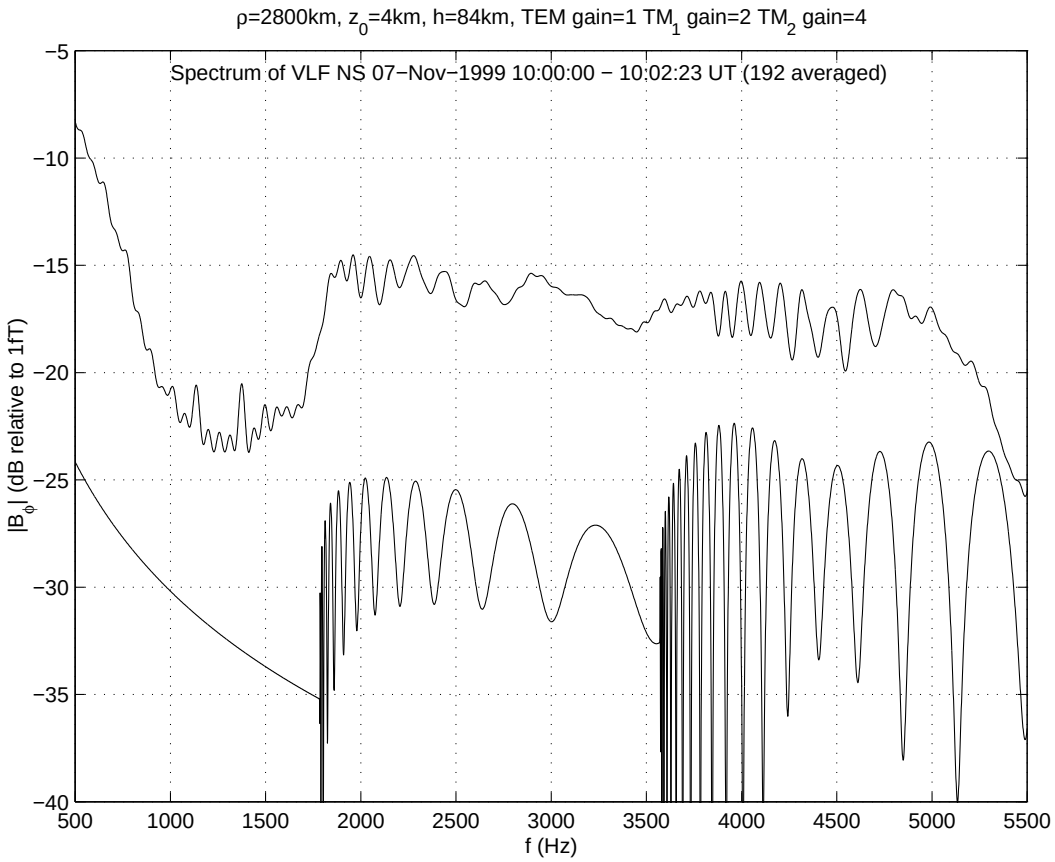
ρ=2800km, z0=4km, h=84km, TEM gain=1 TM1 gain=2 TM2 gain=4
Spectrum of VLF NS 07−Nov−1999 10:00:00 − 10:02:23 UT (192 averaged)
|Bφ| (dB relative to 1fT)
f (Hz)
−5
−10
−15
−20
−25
−30
−35
−40
500
1000
1500
2000
2500
3000
3500
4000
4500
5000
5500

Figure 7:

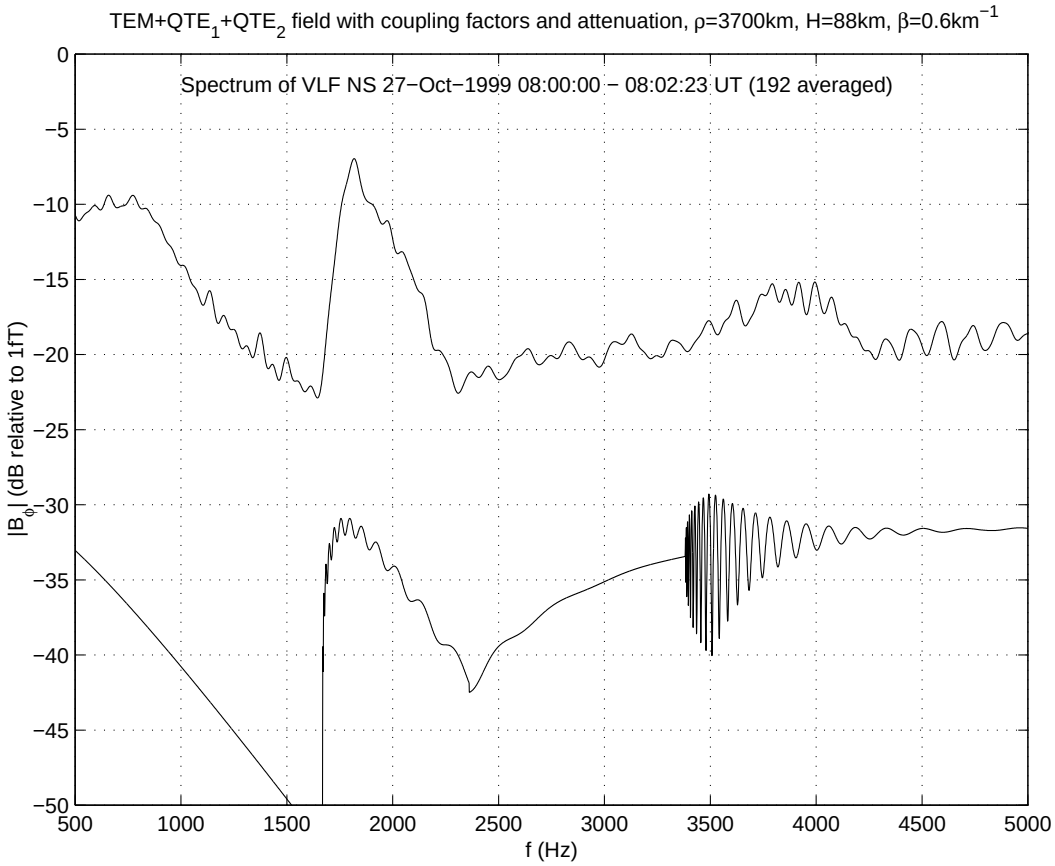
TEM+QTE1+QTE2 field with coupling factors and attenuation, ρ=3700km, H=88km, β=0.6km−1
Spectrum of VLF NS 27−Oct−1999 08:00:00 − 08:02:23 UT (192 averaged)
|Bφ| (dB relative to 1fT)
f (Hz)
0
−5
−10
−15
−20
−25
−30
−35
−40
−45
−50
500
1000
1500
2000
2500
3000
3500
4000
4500
5000

Figure 8: